GRAPHENE OXIDE AND GREEN-SYNTHESIZED REDUCED GRAPHENE OXIDE IN CHITOSAN-BASED NANOCOMPOSITES

Karolina Kosowska*, Patrycja Domalik-Pyzik, Jan Chłopek

AGH University of Science and Technology,
Faculty of Materials Science and Ceramics,
Department of Biomaterials and Composites,
Al. Mickiewicza 30, 30-059 Krakow, Poland
* e-mail: kosowska@agh.edu.pl

Abstract

The first part of the paper concerns synthesis and characterization of two types of nanomaterials: graphene oxide (GO) prepared by modified Marcano method and reduced graphene oxide (rGO) synthesized using green reductant, L-ascorbic acid. Their structural properties were investigated by attenuated total reflection Fourier-transform infrared spectroscopy (ATR-FTIR) and X-ray diffraction (XRD). Results confirmed that L-ascorbic acid is an effective reducing agent. Intensity of the oxygen-groups decreased dramatically what resulted in reduction of the GO interlayer spacing from 0.8 nm to 0.4 nm. The second part of the research was concentrated on the properties of chitosan nanocomposites modified with GO and rGO. Films were prepared by mixing of the chitosan solution with the nanoparticles dispersion. Scanning electron microscopy (SEM) was used to investigate the microstructure of the composites surface. In addition, wettability and pore size of the freeze-dried scaffolds were evaluated. Results of the mechanical tests (increase in Young's modulus) and structural characterization confirmed that chitosan solution and GO dispersion can be mixed homogeneously. Reduction of GO during composite synthesis resulted in better dispersion of the nanosheets what increased surface roughness, wettability and stability in distilled water, PBS and Ringer's solution compared to composite with GO. After detailed biological examination, rGO-modified nanocomposites can be potentially applied in tissue engineering.

Keywords: *graphene oxide, reduced graphene oxide, chitosan, hydroxyapatite, biomaterial*

[Engineering of Biomaterials 142 (2017) 11-16]

Introduction

The suitability of a material for tissue engineering is determined by many factors. Tissue scaffolds have to generate proper chemical and physical signals to be potentially able to transport bioactive molecules and stimulate tissue regeneration. For this reason, researchers are increasingly investigating materials with novel properties. Significant increase in number of studies on graphene and its derivatives has been observed in recent years. Because of its unique properties graphene is a material with great application potential in biomedical field like tissue engineering [1], bioimaging [2], biosensor [3] and drug delivery [4].

Graphene is a monolayer of carbon atoms with sp^2 hybridization. Each atom has three σ-bond and one delocalized π-bond thanks to which it connects with three other atoms and creates honeycomb lattice [5]. Two-dimensional (2D) single layer of carbon, thanks to atomic structure and remarkable electron mobility, possesses great mechanical properties [6], high electrical [7] and thermal conductivity [8], large surface area, and chemical stability [9].

In practice, graphene is defined as a mono-, bi- or multi-layer of sheets. Above the number of ten sheets its properties change rapidly and material behaves more like graphite [10]. Graphene oxide is a one of graphene derivatives, obtained by chemical oxidation. The structure of GO consists of graphene layer with functional groups attached to the surface [11]. Number and type of oxygen groups like hydroxyl, epoxide and carboxyl groups determine the properties of graphene oxide [12]. Thanks to its reactive groups, GO can interact with polymer matrix and form stable colloidal emulsion in polar solvents [11,13]. It has been reported that GO promotes proliferation of various types of cells [1,14] and exhibits antibacterial activity [15]. The most common way of GO preparation is Hummers method [16] and its modifications. Graphite flakes are oxidized using $NaNO_3$ and $KMNO_4$ dissolved in concentrated H_2SO_4. Hummers method was improved by Marcano [17]. In the modified procedure, $NaNO_3$ was eliminated and mixture of H_2SO_4 and H_3PO_4 was introduced. This allowed to synthesize more oxidized and hydrophilic GO and eliminate production of toxic gases (NO_2, N_2O_4).

Reduced graphene oxide (rGO) can be synthesized by chemical, thermal or UV exposure reduction of GO. GO and rGO have different chemical and physical properties [18], rGO is less stable in solution [19] and shows electrical conductivity [20]. It was also reported that GO and rGO affect the cells in different ways [21,22]. Most common rGO synthesis method is chemical reduction of GO sheets using hydrazine (N_2H_4) [23]. However, hydrazine is highly toxic [24] and not suitable for biomedical applications. L-ascorbic acid is nontoxic and effectively reduces GO, hence it can be an alternative reducing agent to hydrazine [25,26].

Recently, modification of polymer matrix with GO and rGO becomes more and more popular due to their favorable mechanical properties, biocompatibility and the fact that both those nanofillers can potentially provide novel properties to the scaffold for tissue engineering. Chitosan is one of naturally occurring polymers with great biocompatibility [27] and biodegradability [28]. However, its applications are limited by low mechanical properties and necessity of cross-linking with e.g. chemical agents. It was reported that graphene derivatives like GO and rGO have positive influence on chitosan physical [29] and biological [13] properties, as well as degradation behaviour [30]. In this work we present simple and green method of GO synthesis (modified Marcano method) and reduction with L-ascorbic acid. Next we investigated the relation between type and content of nanoparticles and the morphology, structure, mechanical properties and degradation behavior of the chitosan-based composite films.

Materials and Methods

Materials

High molecular weight chitosan (M = 600 000 – 800 000 g/mol) with 90% deacetylated was purchased from Acros Organics, USA. Concentrated acetic acid and L-ascorbic acid were purchased from Avantor Performance Materials Poland S.A. Hydroxyapatite (HA) was purchased from Chema-Elektromet, Poland.

Graphene Oxide (GO) was prepared in the Institute of Electronic Materials Technology (ITME), Poland by modified Marcano method, as described previously in [31]. Briefly, oxidation of graphite was carried out by mixing graphite flakes with oxidant agent, potassium permanganate ($KMnO_4$) in the presence of sulfuric acid (H_2SO_4) and phosphoric acid (H_3PO_4). The mixture was kept for 4 hours under vigorous stirring. Next, perhydrol was added. Then the mixture was cooled down and washed with hydrochloric acid (HCl) aqueous solution and distilled water. Material was mechanically exfoliated to obtain flakes as thin as possible. The suspension was freeze-dried.

GO reduction was performed in the water solution of L-ascorbic acid (L-AA) and sodium hydroxide (NaOH). In typical experiment 300 mg of L-AA was added to 300 ml aqueous suspension of GO (0.01 mg/ml). Next, NaOH solution (1M) was dripped to adjust the pH to 9-10. In alkaline conditions GO sheets exhibit the best colloidal stability thanks to the electrostatic repulsion forces. The whole system was sonicated for 1 h, heated to 70°C and kept under vigorous stirring for 2 h. After the reduction, the material was centrifuged and washed with distilled water until the pH was neutral, followed by freeze-drying.

The chitosan/GO composite films were prepared by solution casting method. Known amount of chitosan was dissolved in 5% acetic acid solution and stirred overnight using magnetic stirrer, in ambient conditions. GO flakes were dispersed in 10 ml distilled water and homogenized in ultrasonic bath for 3 h. Next, GO dispersion was gradually added to the chitosan solution, followed by stirring and sonication. The mass content of GO was: 0, 0.5, 1.0, 1.5, 2.0 and 3.0%. Finally solutions were casted onto Teflon dishes and left at room temperature for 96 h. The composite with 1.5% (w/w) rGO content was prepared by adding appropriate amount of the previously prepared rGO to the chitosan solution. Also, chitosan/rGO/hydroxyapatite (HA) (6.0% w/w) composites were fabricated.

Methods

Morphology analysis

Microstructure of the composites was characterized by scanning electron microscopy (SEM) (Nova NanoSEM 200). To measure the pore diameter, the composites were freeze-dried and then cut into thin slices with a scalpel. As prepared porous samples were mounted onto holder and coated with conductive carbon layer prior to SEM analysis.

Structural analysis

The structural properties of the nanoparticles and composite films were investigated by X-ray diffraction (XRD) using X'Pert Pro diffractometer with Cu Kα X-ray sources (λ = 1.5406 Å) and attenuated total reflection Fourier-transform infrared spectroscopy (ATR-FTIR) using Bruker Tensor 27 equipment.

Mechanical properties

Tensile test of the composite films was performed on universal mechanical tester (Zwick 1435). The samples were cut into strips with a dimension of 5 mm x 30 mm; testing speed was 1 mm/min.

Wettability

The contact angle of composite films was measured by sessile drop method (Krüss Drop Shape Analyzer). Ten drops of deionized water were tested for each samples and the average value was calculated.

***In vitro* degradation**

In vitro degradation test of the composites was carried out in distilled water, phosphate buffered saline (PBS), and Ringer's solution. The samples were incubated for 2 months, at 37°C.

Results and Discussions

Characterization of GO and rGO powders

GO, synthesized by oxidation and exfoliation of graphite flakes by modified Marcano method was characterized by ATR and XRD. The FTIR-ATR spectra of GO presented in FIG. 1 shows five main peaks which can be assigned to: O-H groups (3404 cm^{-1}), C=O stretching vibrations of carboxylic groups (1738 cm^{-1}), C=C stretching of the sp^2 network (1662 cm^{-1}), C-O groups in C-OH (1370 cm^{-1}), C-O stretching vibration of C-O-C (1113 cm^{-1}). In the case of rGO, intensity of the peaks decreased dramatically. It confirmed that the oxygen groups can be removed in reduction process using L-ascorbic acid. X-ray diffraction pattern (FIG. 2) of GO shows sharp peak at 11.51° (peak is marked with a black square; rest of the peaks in the pattern come from excipient used for XRD analysis), which completely disappeared after GO reduction and a new wide peak showed up at 22.83°.

The interlayer spacing of the GO powder at ~0.77 nm decreased to ~0.39 nm what is the effect of removing oxygen functional groups. During the reduction, the functional groups are removed from the graphene sheets by reacting with the hydrogen atoms from the L-ascorbic acid, and water is produced. Nucleophilic attack and thermal reduction restore C=C bonds. Alkaline conditions ensure electrostatic repulsion of graphene sheets, which hinders π-π stacking between sheets and prevents agglomeration [26].

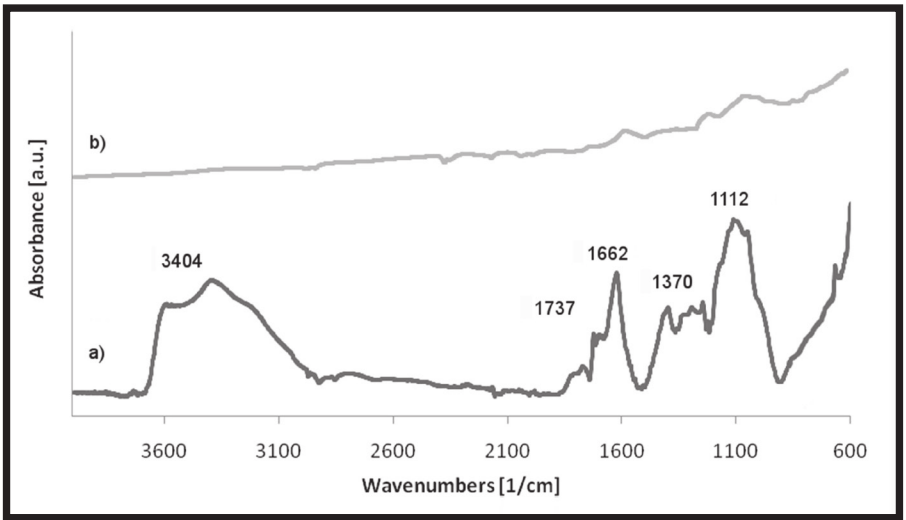

FIG. 1. ATR spectra of: a) GO, b) rGO.

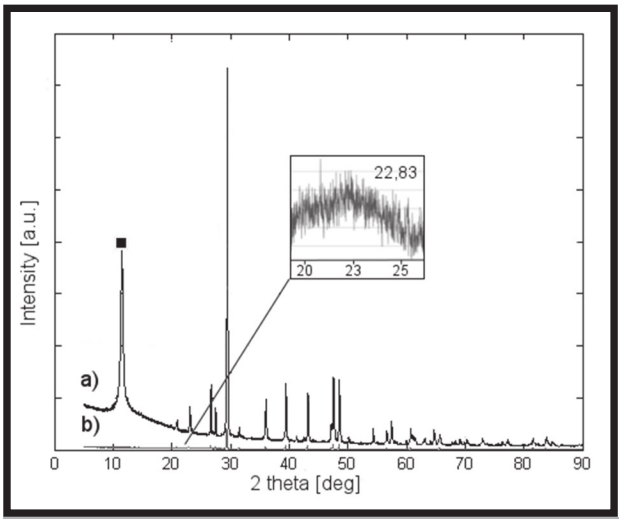

FIG. 2. X-ray diffraction of: a) GO, b) rGO.

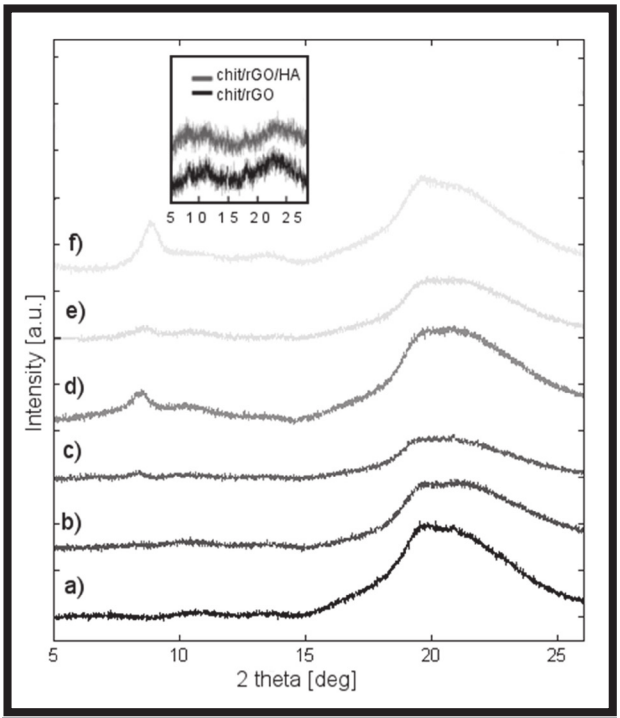

FIG. 3. X-ray diffraction patterns of chitosan: a) pure, b) 0.5% GO, c) 1.0% GO, d) 1.5% GO, e) 2.0% GO, f) 3.0% of GO and films with 1.5% rGO and 6% HA.

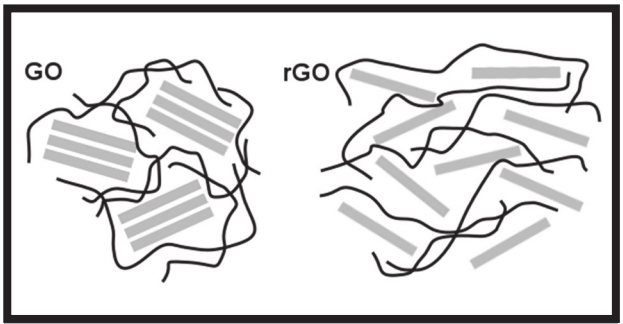

FIG. 4. Schematic representation of behaviour of GO and exfoliated rGO sheets in polymer matrix.

Characterization of the nanocomposites

Chitosan films containing 0.5%, 1.0%, 1.5%, 2.0% and 3.0% of GO were prepared by mixing dispersion of the nanofillers with the polymer solution. Nanocomposites with 1.5% of rGO and 6.0% of HA were also fabricated. Interaction between matrix and fillers, dispersion of graphene derivatives and chitosan crystallinity were analyzed by SEM and XRD.

XRD patterns of chitosan films modified with GO are shown in FIG. 3. Broad peak at 20° is referred to the amorphous structure of pristine chitosan. Weak diffraction peak for the nanocomposites with 1.5%, 2.0% and 3.0% GO can be also seen at 8° and corresponds to the crystalline phase formed as a result of graphene oxide addition. Due to the low content of the nanofiller and good dispersion in the matrix, peaks characteristic for GO are not detected in the composites. The degree of chitosan crystallinity can be calculated on the basis of the peak area according to the formula:

$$x_c = \frac{I_c}{I_c + I_a} \qquad (1)$$

Where I_c is an area of peak corresponding to the crystalline structure and I_a is a peak area of amorphous phase. The crystallinity degree of the nanocomposites was 2.5%, 4.6%, 4.3% and 8.6% for chitosan with 1.0%, 1.5%, 2.0% and 3.0% of GO, respectively. The structure of the pure chitosan and the nanocomposites with 0.5%, 1.0% of GO content was amorphous. The presence of GO in the casted chitosan solution promoted the crystallization process by a nucleation effect.

Nanocomposites with rGO were prepared with the simultaneous reduction of graphene oxide under alkaline conditions that caused electrostatic repulsion of the GO sheets. The volume fraction of the exfoliated, individual rGO sheets dispersed in the polymer matrix were higher than GO, despite the same mass content, and caused the self-organization of the composite (FIG. 4). XRD patterns of the film with rGO present very weak, broad peaks (FIG. 3). Reduction of GO increased the surface area and volume of the nanofiller in the matrix. Chitosan chains attached to the surface of the rGO sheets due to the physical interaction.

SEM analysis of the surface morphology clearly showed differences between composites with GO and rGO (FIG. 5). Surface of the pristine chitosan was homogeneous and smooth (FIG. 5a). In the case of the films with GO, the surface roughness increased with the mass content of the filler (FIG. 5b, c, d). However, the surfaces were still quite smooth, which was due to the low content of GO and low exfoliation of GO sheets. On the other hand, surfaces of the films with rGO were rough and a lot of rGO sheets were visible (FIG. 5e). As shown in FIG. 5f, homogenously dispersed HA particles, densely planted surface of the film, further increasing roughness what can potentially improve cells adhesion.

Samples after freeze-drying were cut into slices to analyze the shape and pore size under SEM as shown in FIG. 6. The pore diameter of pristine chitosan was in the range of 100-150 μm. The pores formed a dense network of interconnected channels. Introduction of GO reduced the pore diameter but did not affect their shape. Pore walls remained thin and smooth (FIG. 6a, b). Significant differences are seen for the samples with rGO. Pores are bigger, with diameter around 200 μm (FIG. 6.c, e) and their walls are thick and rough (FIG. 6d, f). During the manufacture of the composites with the simultaneous reduction of GO, chitosan chains attached to the exfoliated rGO sheets, connecting them together and forming thick wall with rough surface.

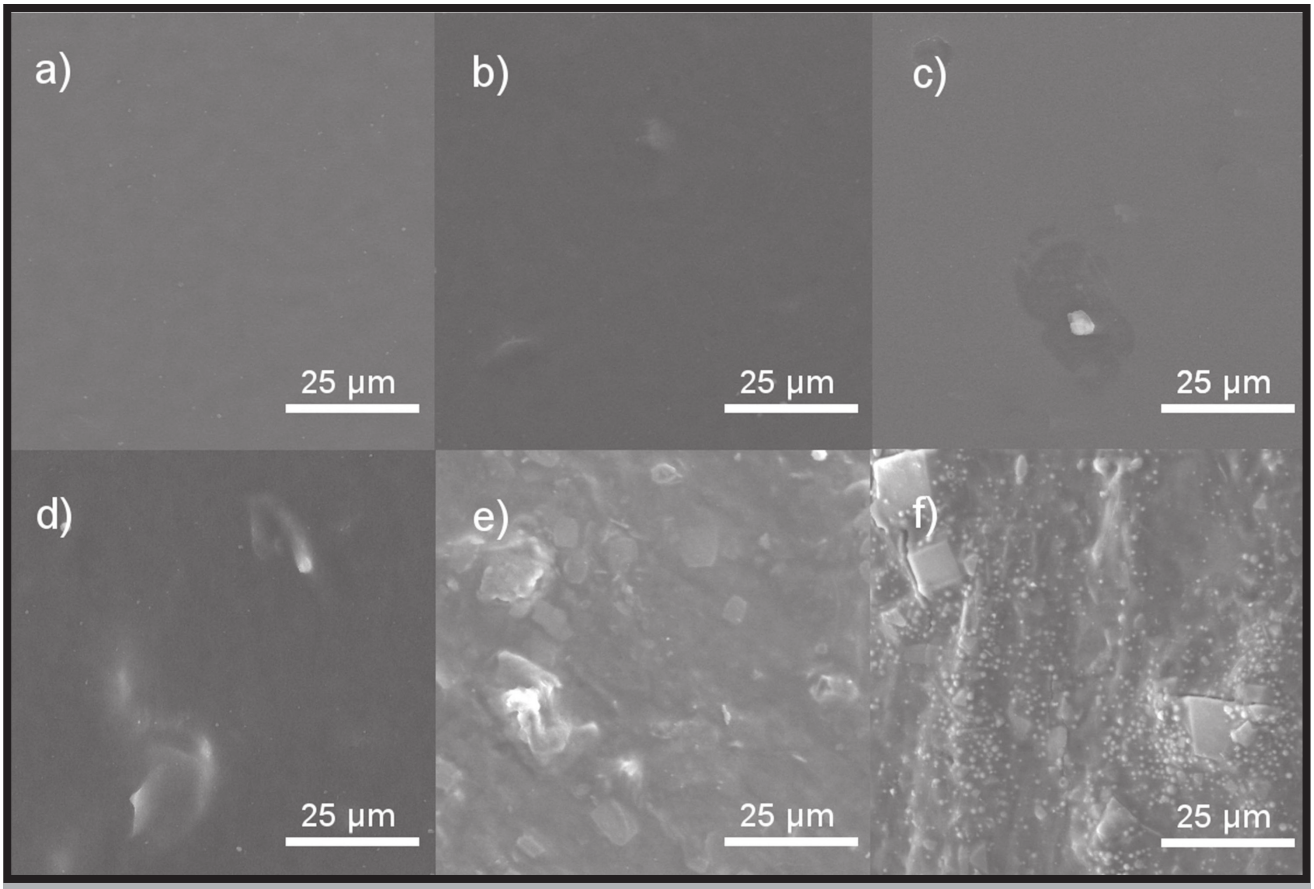

FIG. 5. SEM images of chitosan film microstructure: a) pure, b) with 0.5% GO, c) 1.5% GO, d) 3.0% GO, e) 1.5% rGO, f) 1.5% rGO and 6.0% HA.

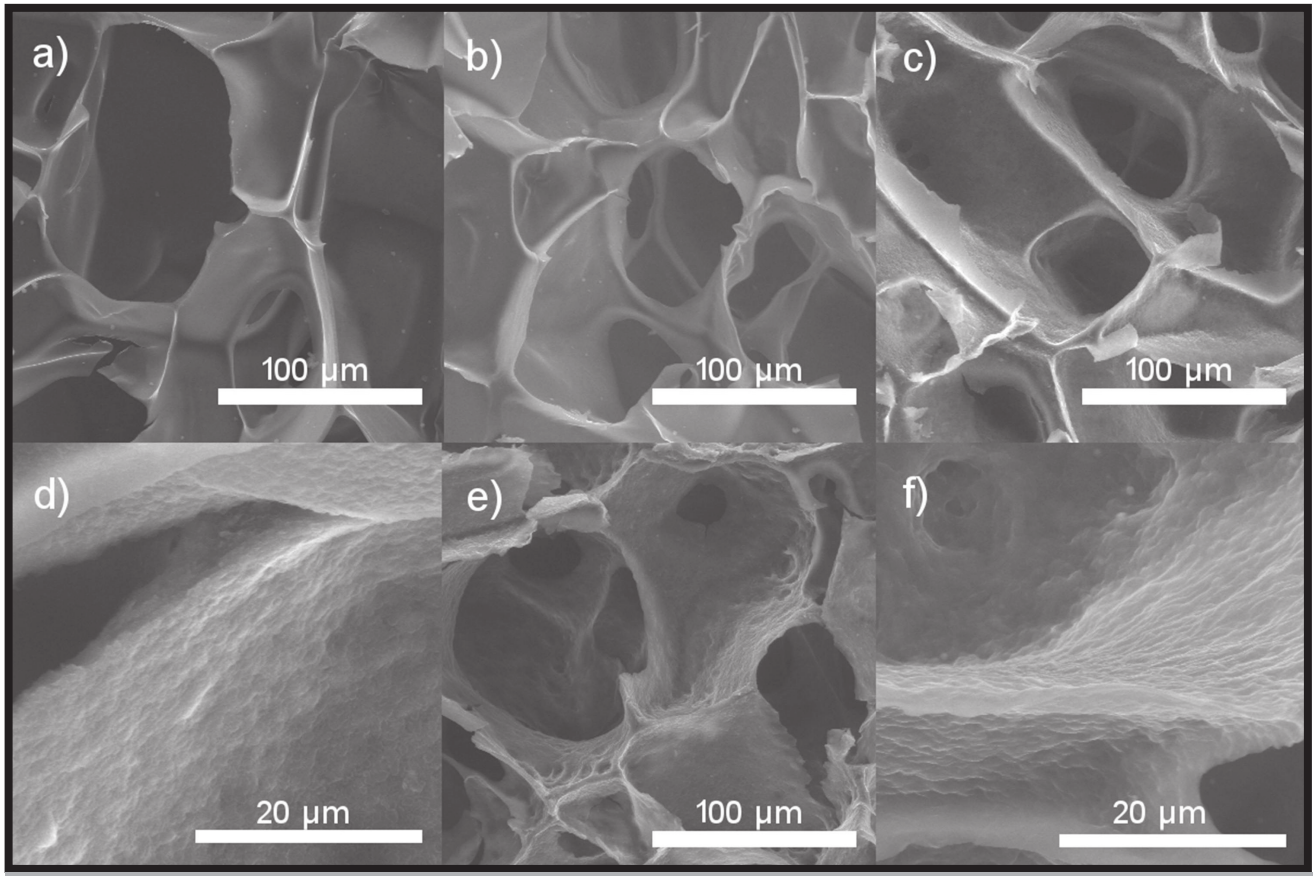

FIG. 6. SEM images of a) chitosan b) chitosan/1.5% GO, c,d) chitosan/1.5% rGO, e,f)) chitosan/1.5% rGO/6.0% HA.

TABLE 1. Properties of chitosan and nanocomposites modified with GO, rGO and HA (mean ± SD).

Sample	Average pore diameter [μm]	Contact angle [deg]	Young's modulus [MPa]
Chitosan	117 ± 34	110 ± 22	2035 ± 156
Chitosan/0.5% GO	86 ± 22	106 ± 2	1851 ± 213
Chitosan/1.0% GO	68 ± 16	91 ± 2	2296 ± 391
Chitosan/1.5% GO	68 ± 19	103 ± 4	2749 ± 253
Chitosan/2.0% GO	60 ± 14	96 ± 2	2341 ± 58
Chitosan/3.0% GO	60 ± 15	85 ± 3	1369 ± 17
Chitosan/1.5% rGO	184 ± 29	75 ± 4	443 ± 99
Chitosan/1.5% rGO/6.0% HA	204 ± 25	65 ± 4	803 ± 76

TABLE 2. Weight loss of composites with rGO and HA (mean ± SD).

Solution	Weight loss [%]			
	Chitosan/1.5% rGO		Chitosan/1.5% rGO/6.0% HA	
	1 month	2 month	1 month	2 month
Distilled water	55 ± 3	58 ± 3	53 ± 2	56 ± 3
PBS	47 ± 2	53 ± 3	45 ± 2	52 ± 3
Ringer	42 ± 2	48 ± 2	46 ± 2	57 ± 3

The average pore diameter for all types of the scaffolds is summarized in TABLE 1. The scaffold for bone regeneration must be highly porous and the pores should create a network to allow cell infiltration and diffusion of nutrients, waste and oxygen. Another advantage is the roughness of the walls, which can facilitate cells adhesion. The pore diameter should not be less than about 200 μm [32]. From this perspective, the composite scaffolds with rGO, and rGO with HA were found as most suitable for application in tissue engineering.

Another important factor that determines the attachment of the cells to the scaffold's surface is appropriate wettability. High contact angle of the chitosan is due to its hydrophobic nature. When the content of GO increases, the contact angle decreases (TABLE 1), improving the hydrophilicity. This is an effect of the increased surface roughness and the presence of hydrophilic functional groups on the GO sheets. However, the addition of 1.5% GO reduced the contact angle by only 7°. The surface of the film was still smooth and nanofillers were rarely seen. The greatest improvement in wettability, resulting in fully hydrophilic character, was observed for composites with rGO. This is due to different process of composite formation. Exfoliated, well-visible under SEM rGO sheets, surrounded by chitosan, created a unique, microscale roughness features on the film surface. In addition, there were many well-dispersed spherical particles on the surface of the film containing HA. This led to a decrease of the water contact angle from 117° to 75° and 65° for chitosan/rGO and chitosan/rGO/HA, respectively.

The mechanical properties of the films were characterized by the uniaxial tensile test. Generally, the composites with GO were tough and fragile. The Young's modulus increased with the nanofiller content up to 2.0%, as shown in TABLE 1. The best enhancement effect was obtained for the composite with 1.5% GO, in which the Young's modulus increased by 35%. Improvement in the mechanical properties can be attributed to the high surface area of the GO sheets and their good dispersion in the polymer matrix. The decrease of the mechanical properties of 3.0% for GO composite can be related to the agglomeration of the filler. Composites modified with rGO behaved differently. They were soft and easy to bend without cracking but at the same time, only small force was needed to break them. The exfoliated, oriented rGO sheets with strong π-π interactions were joined by chitosan chains during the composite fabrication with the simultaneous reduction of GO by L-ascorbic acid. Chemical cross-linkers were not used to create bonds between polymer chains. However, degradation behaviour of the composites showed that rGO could work as physical cross-linking agent and stabilized polymer network. Films containing GO dissolved after one day of incubation at 37°C, thus it can be concluded that the chemical bonds between chitosan and functional groups attached to the nanosheets surface were not created. Composites with rGO showed good stability in all analysed liquids. Weight loss after 1 and 2 months is shown in TABLE 2. Degradation behavior of all the samples was similar. The first stage was faster, the weight of the samples reduced by half; however the samples kept their shape and did not break apart. The second stage was slower and the weight loss for each sample increased by only few percent. There were no significant differences between the composite with rGO only and the composite with rGO and HA.

Conclusions

We presented a simple method of fabrication of chitosan composites with the simultaneous reduction of GO with a non-toxic reducing agent, L-ascorbic acid. Chitosan properties like surface wettability, stability during degradation at the human body temperature or pore structure were improved thanks to the rGO addition. Due to the exfoliation of the nanosheets and their uniform distribution, hydrogels exhibited properties potentially useful in tissue engineering. Further tests, including biocompatibility and antibacterial activity evaluation are necessary.

Acknowledgments

Joanna Jagiełło and Dr. Ludwika Lipińska from the Institute of Electronic Materials Technology (ITME) in Warsaw are gratefully acknowledged for providing graphene oxide. This research was financed by the grant No 15.11.160.019 (Faculty of Materials Science and Ceramics, AGH UST). The National Centre for Research and Development, Poland is gratefully acknowledged for providing financial support under STRATEGMED program: grant No. STRATEGMED3/303570/7/NCBR/201.

References

[1] Shin, S. R. et al.: Graphene-based materials for tissue engineering. Advanced Drug Delivery Reviews 105 (2016) 255-274.
[2] Lin, J., Chen, X. & Huang, P.: Graphene-based nanomaterials for bioimaging. Advanced Drug Delivery Reviews 105 (2016) 242-254.
[3] Justino C.I.L., Gomes A.R., Freitas A.C., Duarte A.C., Rocha--Santos T.A.P.: Graphene based sensors and biosensors. TrAC Trends in Analytical Chemistry 91 (2017) 53-66.
[4] Zhang, Q. et al.: Advanced review of graphene-based nanomaterials in drug delivery systems: Synthesis, modification, toxicity and application. Materials Science and Engineering: C 77 (2017) 1363-1375.
[5] Georgantzinos S.K., Giannopoulos G.I., Fatsis A., Vlachakis N.V.: Analytical expressions for electrostatics of graphene structures. Physica E: Low-dimensional Systems and Nanostructures 84 (2016) 27-36.
[6] Lee C., Wei X., Kysar J.W., Hone J.: Measurement of the Elastic Properties and Intrinsic Strength of Monolayer Graphene. Science 321 (2008) 385-388.
[7] Wu Z.-S. et al.: Synthesis of Graphene Sheets with High Electrical Conductivity and Good Thermal Stability by Hydrogen Arc Discharge Exfoliation. ACS Nano 3 (2009) 411-417.
[8] Balandin, A. A. et al.: Superior Thermal Conductivity of Single--Layer Graphene. Nano Letters 8 (2008) 902-907.
[9] Sharon M., Sharon M.: Graphene: an introduction to the fundamentals and industrial applications. Wiley (2015)
[10] Geim A.K., Novoselov K.S.: The rise of graphene. Nature Materials 6 (2007) 183-191.
[11] Dreyer D.R., Park S., Bielawski C. W., Ruoff R.S.: The chemistry of graphene oxide. Chem. Soc. Rev. 39 (2010) 228-240.
[12] Yan J.-A., Chou M.Y.: Oxidation functional groups on graphene: Structural and electronic properties. Physical Review B 82 (2010).
[13] Pandele A.M. et al.: Preparation and in vitro, bulk, and surface investigation of chitosan/graphene oxide composite films. Polymer Composites 34 (2013) 2116-2124.
[14] Kim T.-H., Lee T., El-Said W., Choi J.-W.: Graphene-Based Materials for Stem Cell Applications. Materials 8 (2015) 8674-8690.
[15] Liu S. et al.: Antibacterial Activity of Graphite, Graphite Oxide, Graphene Oxide, and Reduced Graphene Oxide: Membrane and Oxidative Stress. ACS Nano 5 (2011) 6971-6980.
[16] Hummers W.S., Offeman R.E.: Preparation of Graphitic Oxide. Journal of the American Chemical Society 80 (1958) 1339-1339.
[17] Marcano D.C. et al.: Improved Synthesis of Graphene Oxide. ACS Nano 4 (2010) 4806-4814.
[18] Pei S., Cheng H.-M.: The reduction of graphene oxide. Carbon 50 (2012) 3210-3228.
[19] Konios D., Stylianakis M.M., Stratakis E., Kymakis E.: Dispersion behaviour of graphene oxide and reduced graphene oxide. Journal of Colloid and Interface Science 430 (2014) 108-112.
[20] Li Z.J., Yang B.C., Zhang S.R., Zhao C.M.: Graphene oxide with improved electrical conductivity for supercapacitor electrodes. Applied Surface Science 258 (2012) 3726-3731.
[21] Kang Y. et al.: Graphene oxide and reduced graphene oxide induced neural pheochromocytoma-derived PC12 cell lines apoptosis and cell cycle alterations via the ERK signaling pathways. International Journal of Nanomedicine 12 (2017) 5501-5510.
[22] Katsumiti A., Tomovska R., Cajaraville M.P.: Intracellular localization and toxicity of graphene oxide and reduced graphene oxide nanoplatelets to mussel hemocytes in vitro. Aquatic Toxicology 188 (2017) 138-147.
[23] Park S. et al.: Hydrazine-reduction of graphite- and graphene oxide. Carbon 49 (2011) 3019-3023.
[24] Guldberg Klenø T. et al.: Mechanisms of hydrazine toxicity in rat liver investigated by proteomics and multivariate data analysis. PROTEOMICS 4 (2004) 868-880.
[25] Zhang J. et al.: Reduction of graphene oxide via L-ascorbic acid. Chem. Commun. 46 (2010) 1112-1114.
[26] Xu C. et al.: Fabrication and Characteristics of Reduced Graphene Oxide Produced with Different Green Reductants. PLOS ONE 10, e0144842 (2015).
[27] Croisier F., Jérôme C.: Chitosan-based biomaterials for tissue engineering. European Polymer Journal 49 (2013) 780-792.
[28] Landriscina A., Rosen J., Friedman A.J.: Biodegradable chitosan nanoparticles in drug delivery for infectious disease. Nanomedicine 10 (2015) 1609-1619.
[29] Yadav S.K. et al.: Mechanically Robust, Electrically Conductive Biocomposite Films Using Antimicrobial Chitosan-Functionalized Graphenes. Particle & Particle Systems Characterization 30 (2013) 721-727.
[30] Depan D., Shah J.S., Misra R.D.K.: Degradation mechanism and increased stability of chitosan-based hybrid scaffolds cross--linked with nanostructured carbon: Process–structure–functional property relationship. Polymer Degradation and Stability 98 (2013) 2331-2339.
[31] Jaworski S., Sawosz E., Kutwin M., et al.: In vitro and in vivo effects of graphene oxide and reduced graphene oxide on glioblastoma. International Journal of Nanomedicine 10 (2015) 1585-1596.
[32] Levengood S.L., Zgang M.: Chitosan-based scaffolds for bone tissue engineering. Journal of Materials Chemistry B 2(21) (2014) 3161-3184.